Impact of reflective materials on urban canyon albedo, outdoor and indoor microclimates

Agnese Salvati [a*], Maria Kolokotroni [a], Alkis Kotopouleas [b], Richard Watkins [b], Renganathan Giridharan [b], Marialena Nikolopoulou [b]

a Brunel University London, Kingston Lane, Uxbridge, Middlesex UB8 3PH, United Kingdom

b University of Kent, Giles Ln, Canterbury, CT2 7NZ, United Kingdom

*Corresponding author

email: agnese.salvati@brunel.ac.uk, Postal address[1]:CSEF Jacques Elliot Annex, Brunel University London, Uxbridge, Middlesex, UB8 3PH, UK

Co-authors emails:

Maria Kolokotroni: maria.kolokotroni@brunel.ac.uk

Alkis Kotopouleas: A.G.Kotopouleas@kent.ac.uk

Richard Watkins: r.watkins@kent.ac.uk

Renganathan Giridharan: G.Renganathan@kent.ac.uk

Marialena Nikolopoulou: M.Nikolopoulou@kent.ac.uk

Abstract

The urban canyon albedo (UCA) quantifies the ability of street canyons to reflect solar radiation back to the sky. The UCA is controlled by the solar reflectance of road and façades and the street geometry. This study investigates the variability of UCA in a typical residential area of London and its impact on

[1]Present address: Barcelona School of Architecture ETSAB UPC, Av. Diagonal, 649, 08028 Barcelona, Spain. agnese.salvati@upc.edu

outdoor and indoor microclimates. The results are based on radiation measurements in real urban canyons and on a 1:10 physical model and simulations using ENVImet v 4.4.6 and EnergyPlus. Different scenarios with increased solar reflectance of roads and façades were simulated to investigate the impact on UCA and street level microclimate. The results showed that increasing the road reflectance has high absolute and relative impact on UCA in wide canyons. In deeper canyons, the absolute impact of the road reflectance is reduced while the relative impact of the walls' reflectance is increased. Results also showed that increasing surface reflectance in urban canyons has a detrimental impact on outdoor thermal comfort, due to increased interreflections between surfaces leading to higher mean radiant temperatures. Increasing the road reflectance also increases the incident diffuse radiation on adjacent buildings, producing a small increase in indoor operative temperatures. The findings were used to discuss the best design strategies to improve the urban thermal environment by using reflective materials in urban canyons without compromising outdoor thermal comfort or indoor thermal environments.

Keywords

Urban albedo, urban canyon, reflective materials, urban microclimate, outdoor thermal comfort, solar radiation

1. Introduction

Managing heat in buildings and cities is one of the priorities of the next decades considering the overlapping effects of climate change, the urban heat island and urban population growth [1–3]. Global and urban warming have a detrimental impact on outdoor thermal comfort, building overheating and heat-related health issues even in cities of high latitudes such as London (Lat 51.5° N) [4,5]. The health risks for the population are higher in cities, where heatwaves are amplified in magnitude and duration due to synergy with the urban heat island (UHI) effect [6–8].

One cause of the UHI effect is the enhanced ability of urban structures to absorb solar radiation compared to rural areas [9–11]. For this reason, one strategy to mitigate the UHI intensity is to increase the albedo of urban surfaces, i.e. the ability to reflect solar radiation back to the sky [12]. This can be achieved by replacing conventional materials for roofs and paving with 'cool materials', having high solar reflectance and infrared emittance [13]. By decreasing solar absorption, cool materials have a beneficial effect on the daytime surface temperature and, consequently, a mitigating effect on urban air temperature, especially when adopted at the neighbourhood and urban scales [13–17]. Using cool materials on the building envelope also reduces the heat transfer through walls and roofs, with beneficial effect on the indoor thermal conditions in summer [18–22]. However, some studies highlighted that increasing the reflectance of roads and façades may have a detrimental impact on street-level microclimate and building cooling loads, due to the increase of reflected radiation towards pedestrians and adjacent buildings [23–26]. This means that increasing urban albedo may have contrasting outcomes at the urban and the micro scales and precautions should be taken before adopting this UHI mitigation strategy at large scale.

Furthermore, most of the state of the art on urban albedo is based on studies using conceptual models of urban areas, where urban geometry is simplified to regular patterns of urban canyons or cubic buildings and the spatial distribution of reflectances of façades and roads is assumed to be homogenous [23, 27–31]. Studies considering the impact of real-world urban geometries and realistic distribution of materials on urban albedo are very limited. For these reasons, a more detailed analysis of the net impact of cool materials in urban settings is needed to understand their actual potential to improve urban microclimate and thermal comfort.

The present study investigates the multiple and interconnected consequences of increasing the solar reflectance of façades and roads at London's latitude (51.5˚N) on: 1) urban canyon albedo, 2) street-level microclimate and outdoor thermal comfort and 3) building indoor thermal conditions. Different spatial distributions of solar reflectances within urban canyons and different canyon geometries are analysed using measurements and simulations by ENVImet and EnergyPlus. The results are discussed to highlight the influence of different spatial distribution of solar reflectances on urban albedo and ground-level microclimate and thermal comfort. The findings can be easily converted into design guidelines for a more informed use of cool materials in the built environment by planners, architects and engineers in London and cities of similar latitudes.

2. Background and state of the art

2.1. Surface albedo, urban albedo and urban canyon albedo: concepts and scale of analysis

The albedo quantifies the reflecting power of a surface on a scale from 0 to 1. In urban climatology, the albedo can be quantified at different scales: at the local-urban scale for the whole urban surface (i.e. urban fabric) or at the scale of individual facets (i.e. roads, façades, roofs) [9]. The reflecting power of individual facets is expressed in terms of surface albedo – or solar reflectance (SR) – given by the ratio of the reflected to the incident solar radiation over a horizontal plane. Measured SR can reach values up to 0.95 for advanced ultra-white materials [32] or be as low as 0.05 for dark materials such as fresh asphalt [12].

Urban surfaces have lower reflecting power due to urban roughness, which causes a trapping of solar reflections, resulting in increasing solar absorption by 10-40% compared to planar surfaces of the same material [31, 33–35]. For this reason, the concept of urban albedo (UA) was introduced in climatology to characterise the ability of the urban surface to reflect radiation back to the sky, considering the combined effect of materials' reflectances and urban form occlusivity [9,12,34]. UA is defined as the ratio of the reflected to the incoming shortwave radiation at the upper edge of the urban canopy layer [27], namely the atmospheric layer extending from ground level to just above roof level. Due to the impact of urban geometry, the typical range of variation of UA is reduced to approximately 0.2 - 0.4.

Urban albedo can also be investigated at the microscale, for individual urban canyons [23]. At this scale, the Urban Canyon Albedo (UCA) is defined as the ratio of the reflected to the incoming radiation at the eaves level of street canyons, corresponding to the intersection of the roof plane with the external walls (theoretical plane illustrated in Figure 1).

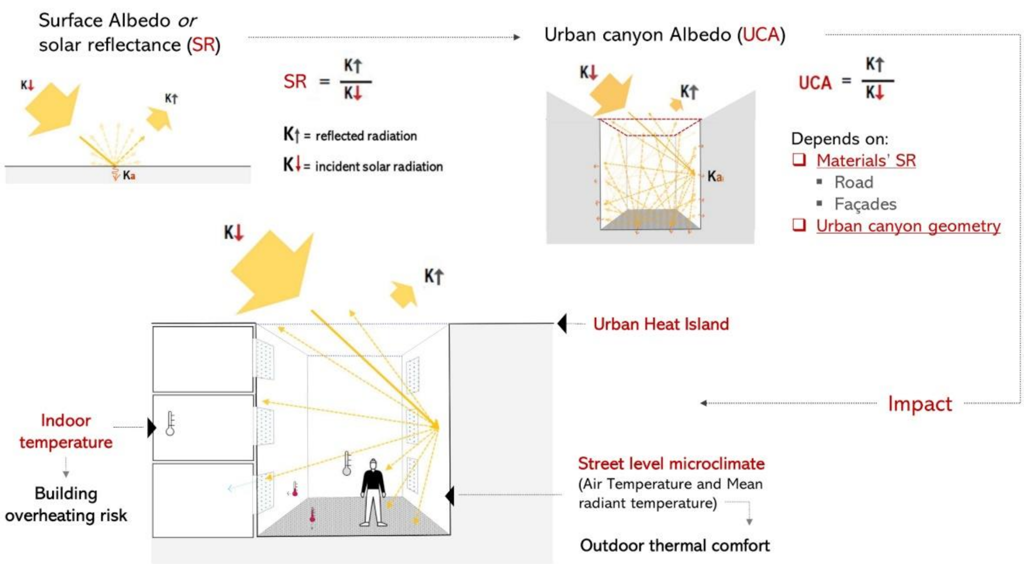

Figure 1 Interconnections between surface albedo, urban canyon albedo, outdoor thermal comfort and building indoor thermal environment investigated in this study. (2 columns picture)

This albedo measure is influenced by the reflectance of façades and roads and the canyon aspect ratio, namely the building height divided by the street width (H/W). The UCA is even lower than the UA because it excludes the contribution of reflected radiation by roof surfaces. The UCA for streets with conventional materials is generally below 0.2 and it can reach extremely low values up to 0.01 in deep geometries (H/W >2) [12]. This scale of analysis is useful to analyse the impact of high reflectance materials on street-level microclimate and indoor environments.

2.2. Quantifying urban albedo: methods and key parameters

The experimental investigation of urban albedo in real urban geometries is very complex. Measurements by aircraft-borne sensors and ground based sensors are not reliable due to the influence of the polluted urban atmosphere in the former and reduced view factor of the urban surface in the latter case [36]. For these reasons, previous experimental studies on UA used simplified scale models.

One important experiment was carried out by Aida [34] at the Yokohama National University (Lat 35˚N) using arrays of concrete blocks (30 cm size per side) arranged in three different configurations. The physical model was equipped with upward and downward facing pyranometers measuring incoming and reflected radiation on top of the model. The experiment showed the UA assumes a U-shaped trend in correlation with time, with minimum at noon and maximum at sunrise and sunset [34]. The experiment also showed that UA decreases when building height or surface irregularity increases. Few other experimental studies have been carried out to investigate UA using physical models of reduced size and uniform material reflectance [23,31,33,37].

More insights into the controlling parameters of UA have been provided by numerical investigations. Yang and Li [27] investigated the relationship between UA and building density parameters for the latitude of Hong Kong (22.3˚N), demonstrating that UA is a minimum in medium density urban areas with building coverage ratio between 0.4 and 0.5. In less dense textures, UA is higher because the higher distance between buildings enhances the ability of urban surfaces to reflect solar radiation back to the sky. UA is higher also in very compact urban textures thanks to the increased contribution of roofs in reflecting radiation out of the urban fabric.

Other studies found that the façade density is also a key parameter of UA, being directly related to the increase of solar interreflections. Groleau and Mestayer [29] showed that UA decreases with increasing façade density, expressed as the total surface of façades divided by the urban area. The importance of the density of vertical surfaces had also been highlighted in a previous numerical study by Aida and Gotoh [38].

Yang et al. [27] and Kondo et al. [39] investigated the impact of building height uniformity, agreeing that higher heterogeneity increases multiple reflections, reducing UA.

Only a few studies analysed the impact of varying surface reflectances on UA. Fortuniak [28] carried out numerical simulations for varying canyon aspect ratios and two surface reflectances. The results showed that urban geometry determines a higher absolute reduction of UA in the model with high reflectance (SR = 0.8), but a higher relative reduction in the model with lower reflectance (SR = 0.4). Steemers et al. [31] tested the impact of urban form and reflectances using 1:500 scale models of a portion of urban fabric of Toulouse, London and Berlin with various surface reflectance coefficients.

For common reflectances of around 20%, the experiment showed that urban geometry reduces solar reflection by 10% in open and up to 40% in more occluded urban forms; for higher reflectances of roads, walls and roofs, the percentage of reflection reduction was smaller.

At the scale of individual canyons, various numerical and experimental studies found that UCA decreases with an increase in the canyon aspect ratio [27–29,36,38,39]. Qin investigated the variability of UCA in relation to the reflectance of roads and walls for different aspect ratios [23]. The study concluded that the canyon aspect ratio plays a primary role in UCA compared to the materials' reflectances and increasing the road reflectivity is effective only in wide canyons with aspect ratio below 1.

2.3. Impact of reflective materials on thermal comfort in urban canyons

The positive impact of higher surface albedo on surface temperature and UHI mitigation has been widely demonstrated in different regions of the world [13,15,17,40–46]. However, a growing number of studies report that increasing the solar reflectance of paving is ineffective or even detrimental on summer outdoor thermal comfort [24,26,47–50]. This happens because, in an urban context, a person is exposed to different types of radiation that contribute to heat the body: incident solar radiation (direct and diffuse), reflected radiation (from the ground and vertical surfaces) and longwave radiation emitted by the sky and the surrounding surfaces. The net impact on the radiant exchange with the body is given by the Mean Radiant Temperature (MRT). For this reason, the MRT is a crucial parameter in the calculation of outdoor thermal comfort indexes such as the Physiological Equivalent Temperature (PET) [51]. Increasing solar reflectance may produce an increase in MRT because the increase in reflected radiation may offset the reduced heat flux emitted from the ground. This explains why reflective materials may have a negative impact on outdoor thermal comfort.

At the building scale, several studies showed that high reflectance materials are effective in reducing building cooling energy demand [19,20,22,52–56]. In an indoor environment, thermal comfort is evaluated using the Operative Temperature, which is derived from air temperature, mean radiant temperature and air speed. In many cases, the calculation can be also approximated to the average of air temperature and MRT (i.e. for low wind speed and no direct sunlight). Using cool materials on the building envelope has a beneficial effect on indoor thermal comfort in summer thanks to the reduction of the indoor MRT produced by the decrease in the external surface temperature.

However, the cooling potential of reflective materials in urban canyons is modified by the interaction between urban and solar geometry. Levinson [57] showed that the effectiveness of cool walls in lowering building cooling demand is reduced in narrow urban canyons due to reduced solar availability to the envelope. Other studies showed that increasing the reflectance of roads and façades may have negative consequences in the buildings' indoor thermal conditions in urban settings, because the reflected radiation is directed toward other buildings more than the sky. For instance, Qin [23] demonstrated that using reflective materials for paving in urban canyons with aspect ratio greater than 1 leads to a significant increase in incident radiation on adjacent façades. Xu at el. [58] showed that increasing the albedo of roads results in a cooling burden for buildings, especially in low-density neighbourhoods. Yaghoobian [59] showed that increasing pavement reflectance from 0.1 to 0.5 increases the cooling loads of an office building up to 11%. Nazarian et al. [25] showed that cool walls can increase solar radiation transmitted into the neighbouring buildings, resulting in higher cooling demands in dense urban areas of Singapore. Colucci at el. [60] also reported a noticeable negative impact of solar interreflections on building cooling loads in urban canyons at the latitudes of Krakow (Lat 50.1˚), Rome (Lat 41.9˚) and Palermo (Lat 38.1˚).

3. Knowledge gap and objectives of the study

The limitations of the reported experimental and numerical studies on UA reflect the simplifications in modelling urban geometry and surface reflectance distribution. None of the cited studies analysed the influence of a more realistic spatial distribution of reflectances of façades and roads on UCA, due to the limited size of the physical models used in experimental studies or to the assumption of one homogenous reflection coefficient for each surface in numerical models. Also, studies investigating the multiple effects of reflective materials at different scales in an urban context are limited. Therefore, the net impact of reflective materials in outdoor and indoor microclimates and thermal comfort is still unclear.

Considering the above discussed issues, this research intended to address the following specific objectives, by taking an urban area of London as case study:

1) An experimental and numerical quantification of UCA in real urban canyons
2) An assessment of the influence of road and façades' materials reflectance and their spatial distribution on UCA
3) An understanding of the impact of high reflectance materials on street-level microclimate and outdoor thermal comfort during heatwaves in urban canyons
4) An assessment of the impact of high reflectance materials on building indoor thermal conditions in urban canyons in summer.

4. Methods

Different techniques and tools were used to achieve the research objectives.

The quantification of UCA was carried out using field measurements in real urban canyons and on a 1:10 physical model of the case study area. The measurements were used to assess the accuracy of the radiation outputs of the new ENVImet IVS algorithm (version 4.4.6), in order to obtain a validated baseline model. Starting from the baseline, different scenarios with varying distribution of the road and façades' materials reflectance were simulated using ENVImet. The results were compared to the baseline model to highlight their impact on UCA and street level microclimate and thermal comfort. Finally, the ENVImet radiation outputs for relevant scenarios were used to force dynamic thermal simulations using Energy Plus to assess the impact on the indoor thermal conditions of buildings in urban canyons. This section presents details of each of these techniques

4.1. Case study area and field measurements

The case study area is located in a typical residential neighbourhood of London, characterised by three storey terraced houses clad with bricks and render of various colours. The extent of the area analysed is approximately 100m by 100m and includes street canyons of similar aspect ratio but different orientation (Figure 2). The average street width is 16m and the average building height is 10m at the eaves and 12m at the ridge level, resulting in a canyon aspect ratio between 0.63 and 0.75.

Spot measurements of the incoming and reflected solar radiation within three urban canyons were performed on the 23rd May 2019. The equipment used was an albedometer (Kipp and Zonen CMA6), composed of two pyranometers, one pointing upward and measuring the incoming radiation from the upper hemisphere and one pointing downward, measuring the reflected radiation from the lower hemisphere. The UCA was calculated as the ratio of the downward to the upward radiation measurement. Measurements were taken in different points and at three heights: street level (1.2m height), 2nd floor level (approximately 5m height) and eaves level (approximately 10m height). A hydraulic platform was used to carry out the measurements at 5 and 10m height (Figure 2).

Figure 2 Views of the case study area and location of the measurements within urban canyons (2 columns picture)

A Bluetooth temperature, humidity and dew point sensor beacon (BlueMaestro Tempo Disc) has also been installed on a lamppost at 5m height from the ground to collect local microclimate hourly data to force ENVImet simulations. This method was found to increase the accuracy of ENVImet air temperature estimations in a preliminary study [61].

4.2. Physical model of the urban area

A 1:10 physical model reproducing the actual geometry and material distribution of the case study area was built at the University of Kent (Canterbury, UK).

The model is located outdoors and equipped with upward and downward facing pyranometers (Hukseflux SR05-A1 with spectral range 285 to 3000 x 10^{-9} m) to measure the incoming and reflected radiation at different points: at the equivalent height of 10 m above roof level (point 1 in Figure 3) and at the eaves level in two urban canyons of the model (Points 2 and 3 in Figure 3).

Figure 3 Views of the 1:10 physical model of the case study area before and after the application the façade colours and details of the pyranometers installed. The circles indicate the location of the pyranometers (2 columns picture)

The reflected radiation measured in point 1 includes the contribution of the roofs and is representative of the local-scale UA. The reflected radiation measured at Points 2 and 3 was used to calculate the UCA as it just included reflections from asphalt, paving and façades. Between July and October 2019, changes were applied to the materials of the model's paving and façades to assess the impact on UCA. The results reported in this study are limited to some representative days: one clear-sky day close to the summer solstice (22 Jun 2019) and the days before and after changes applied to the model (23 Jul, 20 Sept and 6 Oct 2019).

4.3. ENVImet simulations: Index View Sphere (IVS) method for radiation transfer

The microclimate model ENVImet 4.4.6 was used to investigate the impact of varying surface reflectances on UCA, urban microclimate and outdoor thermal comfort.

The radiative fluxes were simulated using the new Indexed View Sphere (IVS) algorithm which calculates the secondary radiative fluxes (reflected shortwave radiation and longwave radiation emitted from objects) with more accuracy with respect to the previous approach based on the "average view factors" (AVF). The new IVS algorithm calculates and stores the view factor of each element seen by each cell and a reference pointer to the particular building, plant and ground surfaces seen. The pointer links the view factors to the actual state of the objects during the simulation (i.e. surface temperature and solar irradiation), allowing calculation of the secondary radiative fluxes in detail. More information on the new IVS is available in a recent publication by the developers [62].

4.3.1. Validation of the ENVImet radiation outputs

The spot measurements on site and the continuous measurements on the physical model were used to validate the ENVImet IVS radiation outputs. To this aim, two different ENVImet models were created to reproduce the real urban area (detailed model) and the simplified physical model (simplified model). The detailed ENVImet model has vegetation and reproduces the same ratio of material distribution as in the case study area (details are provided in the Appendix). Data on urban geometry and spatial distribution of materials were obtained from several site surveys, GIS databases [63] and satellite data (Google Earth). The source for the reflectance coefficients is the London Urban Micromet data Archive 'LUMA' [64]. The simulations to evaluate the IVS algorithm were run for the corresponding days of measurements, by applying an adjustment factor for the global horizontal radiation according to measurements. The ENVImet radiation output "Reflected shortwave radiation lower hemisphere" was compared with the reflected radiation measured at the corresponding points and at the same time in the urban canyons and on the physical model. The Pearson correlation coefficient was used to assess the agreement between calculated and measured UCA.

4.3.2. ENVImet models to simulate scenarios using reflective materials

The detailed model was used as a baseline for the current microclimate conditions in comparison to seven scenarios where the reflectances of façades and paving were changed in different ways. The model dimensions are 200m by 200m (mesh size of 2m), so as to include a sufficient portion of upwind urban area for the correct calculation of urban microclimate conditions avoiding border effects [61]. The changes applied to the three canyons of the urban area are schematically illustrated in Figure 4. The maximum reflectance coefficients for façades and roads were set to 0.6 and 0.5 respectively; higher values were discarded as they would entail glare issues.

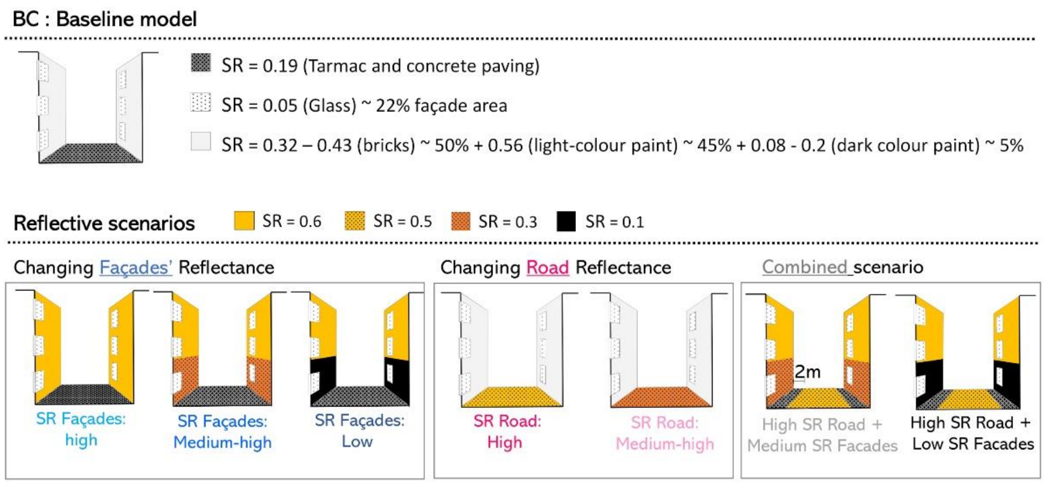

Figure 4 Simulated scenarios with varying solar reflectance (SR) of the façades' and road' materials (2 columns picture)

The performance of the various scenarios was assessed in terms of UCA and outdoor thermal comfort. The UCA potential was assessed by comparing the reflected radiation at the eaves level. The impact on outdoor thermal comfort was analysed considering the change in air temperature, mean radiant temperature (MRT) and Physiological Equivalent Temperature (PET) at the street level (1.5 m height). The PET index was calculated using the BIO-met ENVImet module.

The simulations were forced using the hourly air temperature and relative humidity measured by the sensor installed on the lamppost at the urban site. The forcing data correspond to the 24th and 25th of July 2019, when an intense heatwave occurred in London, with peak air temperature at the urban site up to 37.7 °C. The simulation period was 36 hours. The results were analysed for the last 24hrs, excluding the first 12 hours warm-up period.

Additional simulations were carried out for some relevant scenarios to assess the sensitivity of UCA to the sky conditions and urban canyon geometry. The simulations were forced using measured weather data over 5 days of July characterised by varying sky conditions and for two simplified urban canyon geometries with aspect ratio of 0.75 (as in the case study area) and 1.5 (by doubling the building height). The 5 days simulations were limited to the two simplified geometries given the huge computational power required by the IVS algorithm. To give an idea, the 36 hours simulation using the detailed model and the IVS algorithm lasted approximately 102 hours each, while the 5 days simulation with simple canyon geometry lasted 174 hours, using a high-performance machine with 10 cores and 20 logical processors.

4.4. EnergyPlus simulations using ENVImet outputs

The ENVImet radiation outputs for the 5 days simulation were used as boundary conditions in EnergyPlus to investigate the impact of reflective scenarios on building indoor thermal conditions in urban canyons. The multi-zone EnergyPlus model reproduced the three-story terraced house typology present in the case study area. The same 2-bedroom apartment was modelled on each floor, with the living rooms facing the street, oriented east. Shading surfaces were used in EnergyPlus to reproduce the same canyon geometry modelled in ENVImet (Figure 5). The EnergyPlus model also reproduced the same windows aspect ratio (25%) of the ENVImet models. Internal shades with solar transmittance coefficient equal to 0.4 were used as shading system, assuming they were closed when the incident solar radiation rate on the window exceeded 300 W/m^2. The construction type and thermal performance of the envelope is reported in Table 1.

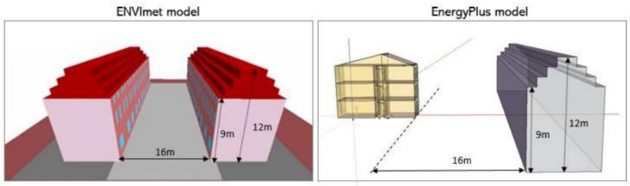

Figure 5 Simple canyon ENVImet model and corresponding EnergyPlus model to investigate the impact of reflective scenarios on the building's indoor thermal conditions (1 column picture)

Table 1 Construction yipe and thermal transmittance (U-value) in the E+ models, for the current and refurbished situation

	Current construction	U-value (W/m2K)	Refurbished construction	U-value (W/m2K)
External wall	*Solid brick* 220m Brick (outer layer) 13mm dense plaster	2.18	*Solid brick, insulated* 19 mm render 60mm high-performance insulation (λ 0.02 W/mK) 220m Brick (outer layer)	0.28
Roof	*Pitched roof* Asphalt shingles roof cavity mineral wool 70mmm plasterboard 12.5 mm	0.45	*Pitched roof, insulated* Asphalt shingles roof cavity 100mm high-performance insulation (λ 0.02 W/mK) plasterboard 12.5 mm	0.18
Exposed floor	*Solid concrete floor* vynil floor finish screed 75 mm Extruded polystyrene 50mm cast concrete 150 mm	0.47	*Solid concrete floor, insulated* vynil floor finish screed 75 mm 80mm high-performance insulation (λ 0.02 W/mK) cast concrete 150 mm	0.22
Glazing	*Double glazing* 3mm Clear glass – 8mm air gap - 3mm clear glass	2.95	*Double glazing* 3mm Clear glass – 8mm air gap - 3mm clear glass	2.95

Source for the current construction type: publicly available EPCs
Materials thermal properties and typical construction from CIBSE Guide A - Appendix 3.A8

Simulations were run for current and refurbished scenarios. The refurbished scenario assumed an improvement in the thermal performance of the building envelope to the current regulations level for London.

The simulation period was the same 5 days of July 2019 used to force ENVImet simulations. The ENVImet BPS output "Diffuse Shortwave Incoming On Façade" was used to calculate an hourly correction factor for the diffuse solar radiation of the EnergyPlus weather file to obtain the same incident radiation in the EnergyPlus building models for each scenario analysed. The solar radiation incoming on façade calculated by ENVImet includes the radiation reflected from the environment. For this reason, the reflection coefficients of ground and shading surfaces in EnergyPlus were set to zero to avoid overestimations of reflections. The impact of the reflective scenarios was assessed considering the changes in the indoor operative temperature of the living room at the middle floor over the five days.

5. Results and discussion

5.1. Measured UCA in the case study area

5.1.1. Field measurements of UCA

The statistical distribution of the UCA measurements taken at different heights within the three urban canyons of the case study area are reported in Figure 6.

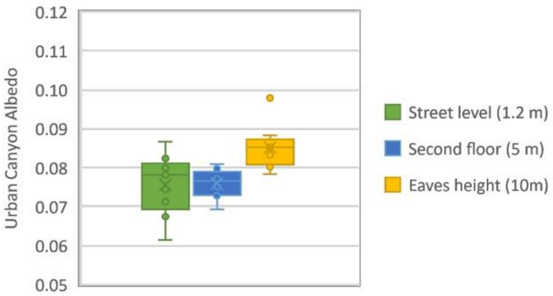

Figure 6 Boxplots of the field measurements of UCA taken in different canyons of the case study area on the 24th May 2019 between 11:20 and 13:50 (British Summer time). The box plots represent the minimum, maximum, median, and the first and third quartiles of the measured data for each measurement height. (1 column picture)

The boxplots are useful to analyse the variation of UCA in different urban canyons and at different heights. The measurements showed a narrow range of variation of the UCA between 0.06 and 0.1

considering all locations. The measured UCA at the street level showed higher variation compared to the second floor and the eaves level. A small but consistent increase in UCA was found at the eaves level compared to the street. However, the measured UCA ranges at the different heights were quite similar: 0.06 - 0.09 at the street level, 0.07 - 0.08 at the second floor and 0.08 – 0.1 at the eaves level. The marginal variation of UCA with height suggests that the horizontal surfaces take a dominant role in those particular geometries and scale. The highest value of UCA (0.1) was recorded at point L2 (Figure 2) at the eaves level. This can be explained by the location of the point facing the façade receiving maximum direct solar radiation at the time of measurements (South South-East oriented façade). The small variation of UCA among the three canyons is explained by the similarities in geometry and material distribution.

5.1.2. Measurements on the physical model

The hourly albedo measured on the physical model is illustrated in Figure 7 for one reference day characterised by high solar radiation and clear sky conditions. The measurements are representative of hourly values of UA (pink dotted line) and UCA (yellow and blue dotted lines). The labels report the daily albedo values, calculated as the ratio of the total reflected to the total incoming shortwave radiation in the measurement point over the day.

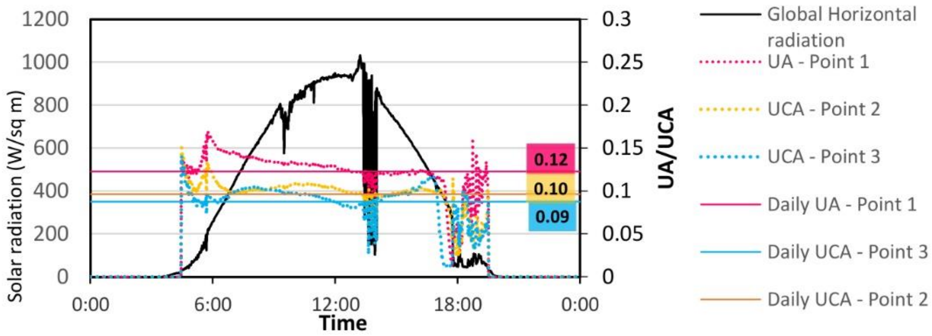

Figure 7 Global horizontal radiation (black line), urban albedo (UA) and urban canyon albedo (UCA) measured on the physical model on the 22 of June 2019. Point one was located on top of the model while points 2 and 3 were located at the eaves level (see Figure 3). (2 columns picture)

The hourly trend of UA confirms the temporal variability with the solar zenith angles, as found in other studies. UA is minimum around noon and maximum for higher zenith angles, in the morning and evening. As expected, the measurements showed that daily UA measured on top of the model (point 1) is higher than UCA, measured at the equivalent height of the buildings' eaves line (points 2 and 3). UA is higher than UCA because it includes the reflected radiation from the roof surfaces.

5.2. Comparing ENVImet radiation outputs with measurements

5.2.1. Comparison with field measurements

The comparison between field measurements and ENVImet outputs is reported in Figure 8. The figure also illustrates the reflected radiation from the lower hemisphere calculated by ENVImet in the whole domain and at the three different heights: street level (0.9m), second floor (5.5m) and eaves level (9.5 m), clearly showing the reduced reflected radiation on top of tree canopies.

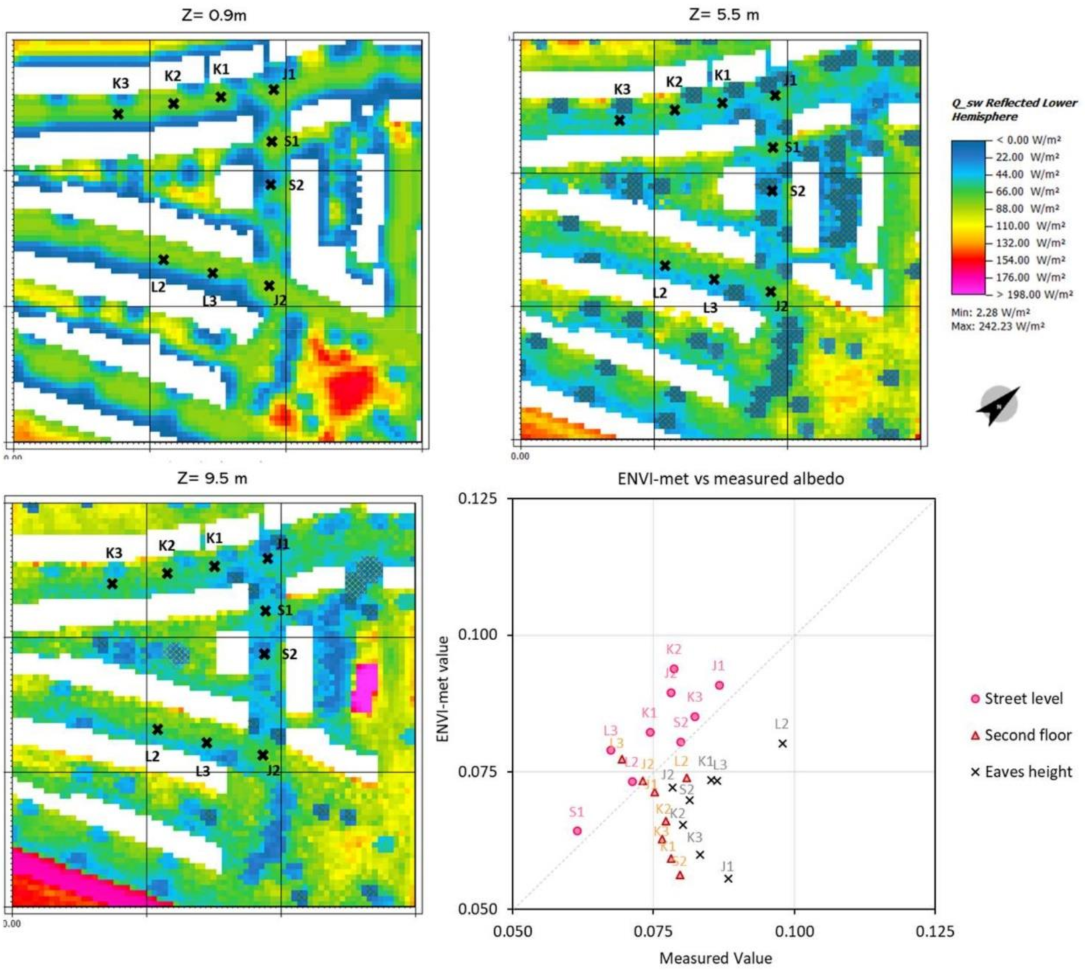

Figure 8 ENVimet reflected radiation and UCA compared to field measurements. (2 columns picture)

ENVImet results showed very good agreement with street-level measurements, with Pearson correlation coefficient of 0.87 ($p < 0.01$), meaning that ENVImet reproduces the spatial variability of solar reflections reasonably well near the ground. The correlations between modelled and measured

UCA at the second floor and eaves level were weaker (Pearson coefficient around 0.1). However, the absolute difference between modelled and measured UCA was below 0.05 in all cases.

It has to be said that such good accuracy in ENVImet simulations can be reached only using the detailed IVS algorithm. When the simplified method is used, the reflections are the same in all the points and overestimated compared to the measurements. Furthermore, substantial differences were found in comparison to the previous version of the IVS algorithm (more details can be found in the Appendix).

5.2.2. Comparison with measurements on the physical model

The comparison between the hourly reflected radiation measured in different points on the physical model and computed by ENVImet is shown in Figure 9. Table 2 reports the average daily UA and UCA in the three measurement points.

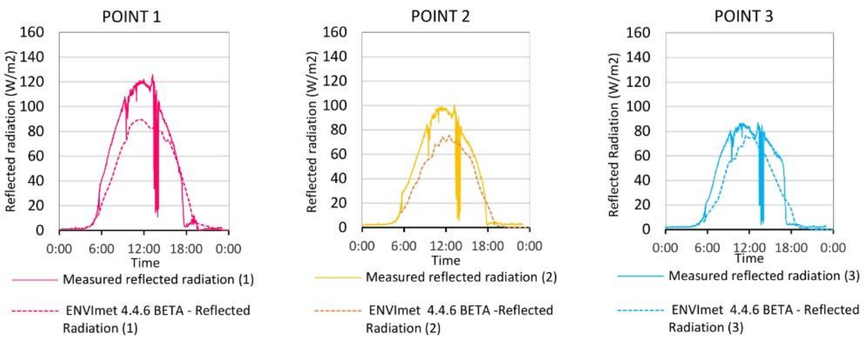

Figure 9 Hourly comparison of the reflected radiation on top of the model (point 1) and at the eaves level (point 2 and 3) calculated by ENVImet and measured on the physical model on the 22nd of June 2019. Refer to Figure 3 for the location of three points. *(2 columns picture)*

Table 2 Daily UA measured on the physical model and calculated by ENVImet

Point 1 (UCA)		Canyon 2 (UCA)		Canyon 3 (UCA)	
Measured	ENVImet 4.4.6	Measured	ENVImet 4.4.6	Measured	ENVImet 4.4.6
0.123	0.090	0.096	0.071	0.088	0.066

The results indicate that ENVImet reproduced quite well the diurnal trend of solar reflections, with a slight underestimation compared to measured data which is maximum at 12pm. The reflected radiation is underestimated both on top of the model (point 1) and at the eaves level of urban canyons (points 2 and 3). However, the daily albedo estimated by ENVImet is very close to measured data, with absolute differences of approximately 0.02 in all three points (Table 2).

The sensitivity of ENVImet to changes in the surfaces reflectances was assessed using measurements on the physical model corresponding to different materials configurations. The results are summarised in Table 3.

Table 3 Impact of materials on canyon albedo: sensitivity of ENVImet and measured data

		Measured *		ENVImet 4.4.6. *	
Model ID and Ref Day	Materials	Daily UCA (point2)	Impact	Daily UCA (point2)	Impact
As built Reference period* 23/07/2019, 11:40 - 16:25	Roof: tiles Façades: red bricks + glass Ground: tarmac	0.10	-	0.09	-
With Paving - Reference period* 20/09/19, 13:00 - 16:40	Roof: tiles Façades: red bricks + glass Ground: tarmac + concrete paving	0.12	23%	0.10	13%
With Façade colours Reference period* 06/10/19, 11:40 - 16:25	Roof: tiles Façades: red bricks + façade colours + glass Ground: tarmac	0.16	56%	0.11	23%

*Correspond to the periods with valid measurements

The measured data showed an increase in UCA compared to the “As built” configuration by 23% after adding the concrete paving and by 56% after adding the façade colours in addition to the paving. ENVImet results also showed an increase in UCA for the same changes in materials’ reflectances, but with reduced impact equal to +15% and +23% respectively. However, this can be also due to the unavoidable geometry differences between the physical model and the ENVImet model, due to the orthogonal mesh constraints and the limited period of comparison.

5.3. Impact of reflective scenarios on urban canyon albedo

The impact of the reflective scenarios on UCA was analysed at the eaves level in the middle point of each urban canyon of the case study area. The hourly UCA values for each scenario for one representative canyon are illustrated in Figure 10. The average daily UCA of each scenario is compared in the bar graphs on the right side. A more detailed horizontal and vertical distribution of solar reflections within the case study area can be found in the Appendix.

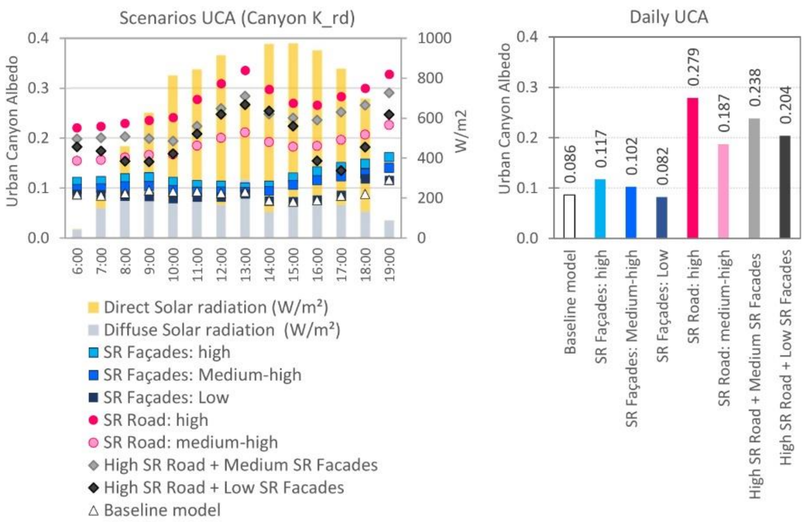

Figure 10 hourly (left) and daily mean (right) urban canyon albedo for the simulated scenarios in different street canyons of the case study area (2 columns picture)

The daily UCA range considering all the scenarios is 0.082- 0.279. The most evident conclusion by comparing the daily results for the different scenarios is that increasing the solar reflectance of roads is much more effective on UCA than increasing façade reflectance. In fact, increasing the reflectance of roads to medium (SR Road: medium-high) and high (SR Road: high) increases the reflection of radiation out of the canyon over the peak irradiation hours, namely between 12:00 and 15:00 British summer time (UTC+1). Conversely, changes in façade reflectance (SR Facades: high, medium-high and low) has a very limited impact on UCA. This can be explained by the reduced solar radiation availability on vertical compared to horizontal surfaces and by the trapping of specular and diffuse reflections from vertical surfaces within the canyon geometry.

The impact of canyon geometry and varying sky conditions on the effectiveness of each strategy is illustrated in Figure 11. The graphs show the daily UCA over six days characterised by different sky conditions and solar irradiation for two canyon geometries with aspect ratio of 0.75 and 1.5.

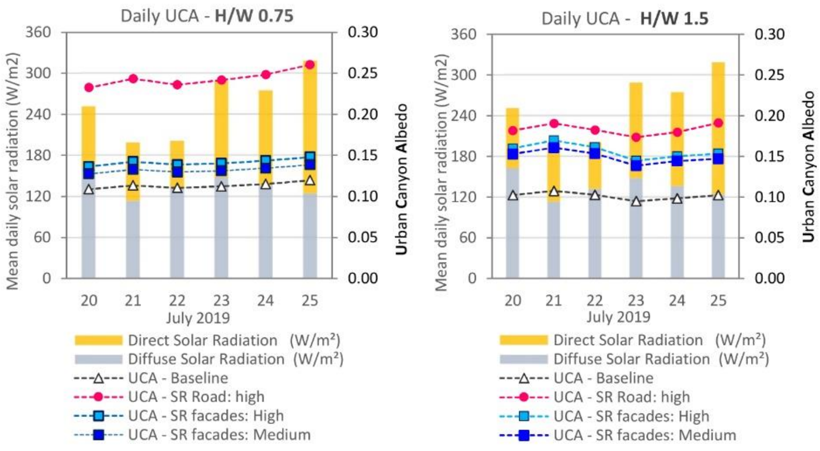

Figure 11 daily UCA varibility for different sky conditions and reflective scenario in two canyon geoemtries with aspect ratio of 0.75 (left) and 1.5 (right) (2 columns picture)

The graphs show that the UCA of street canyons characterised by conventional materials (Baseline) is not much affected by the sky conditions. In both geometries, the UCA of the Baseline configuration remains pretty much constant over the 6 days. Conversely, the scenario with higher reflectivity of the road (SR Road: high) shows an increase in UCA in days with higher solar radiation.

By comparing the two graphs in Figure 11 it is possible to understand the relative impact of material reflectances and canyon geometry on UCA. Doubling the canyon aspect ratio (from 0.75 to 1.5) reduces the UCA for the baseline model by 13-14%. This result was expected, in line with previous studies [27–29,36,38,39]. The impact of deeper urban geometries on UCA is also clear for the scenario with higher road reflectivity (SR Road: high), which is much more effective in increasing UCA of low aspect ratio canyons (0.75) compared to deeper ones (1.5). Conversely, changing the reflectivity of façades has a relatively higher impact on UCA in the deeper canyon. Similar results were found by Qin [23]. Furthermore, the scenarios with high reflectivity of the whole façade (SR Façades: high) or the top half of the façade (SR Façades: medium-high) show higher UCA in deeper canyons compared to shallow ones. This result was unexpected and highlights the relevance of both canyon geometry and solar reflectance distribution in determining the effectiveness of different strategies to increase UCA.

5.4. Impact of scenarios on outdoor thermal comfort

The potential of reflective scenarios to reduce heat stress was analysed over the heatwave peak of the 25th of July 2019, reached at 1pm with a temperature of 37.7 ˚C. The spatial distribution of the PET index was used to assess outdoor thermal comfort in the baseline configuration and for the different scenarios. The PET temperature indicates the equivalent temperature in a typical indoor setting (without wind and solar radiation) that would lead to the same heat balance for the human body [51]. The spatial distribution of PET at 1.5m heigh during the heatwave peak is illustrated in Figure 12 for the baseline configuration. The figure clearly indicates that the most comfortable spots are the vegetated courtyards (i.e. point 5 in Figure 12) and the areas in the shadow of trees or buildings.

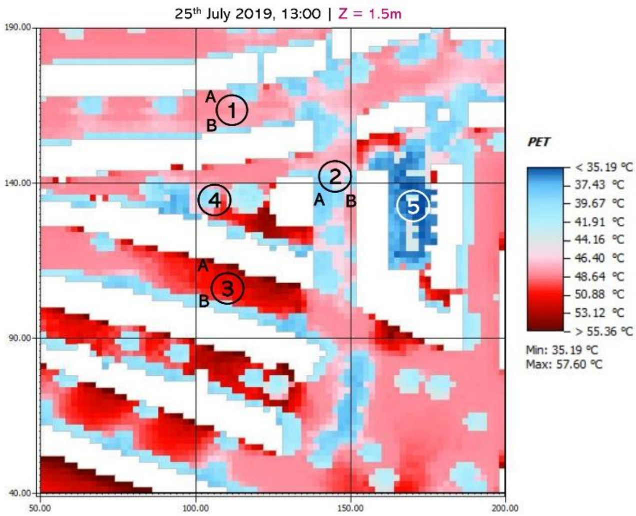

Figure 12 Spatial distribution of the PET at 1.5m above street level during the heatwave peak temperature (1 column picture)

The graph in Figure 13 compares the hourly PET in the three urban canyons and in the vegetated courtyards over the two days of simulation (24-25th July).

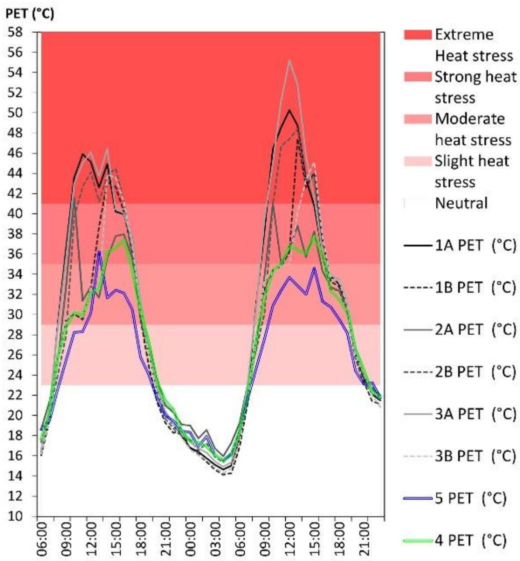

Figure 13 Hourly PET in different points of the case study area (refer to Figure 12 for the locations). The red shadows mark the PET thresholds for thermal stress. The dotted lines in green and blue are vegetated areas while the other lines in grey are points within urban canyons. (1 column picture)

The graphs show that heat stress is mitigated in the green courtyards thanks to the combined beneficial effect of higher soil permeability and solar absorption and shade by trees on air temperature and MRT. The PET is always higher in street canyons, reaching very high values up to 55.2˚C in Canyon 3, indicating a high risk of severe heat stress during heatwave events even in temperate climate regions such as London. The most favourable position within canyons is in the shade of trees (point 2 A in Figure 12). The shadows from buildings also have a positive impact on outdoor thermal comfort, but less effective than shade of trees and vegetated areas.

The changes in the street-level air temperature, MRT and PET determined by an increase in reflectivity of roads and façades are reported in Figure 14.

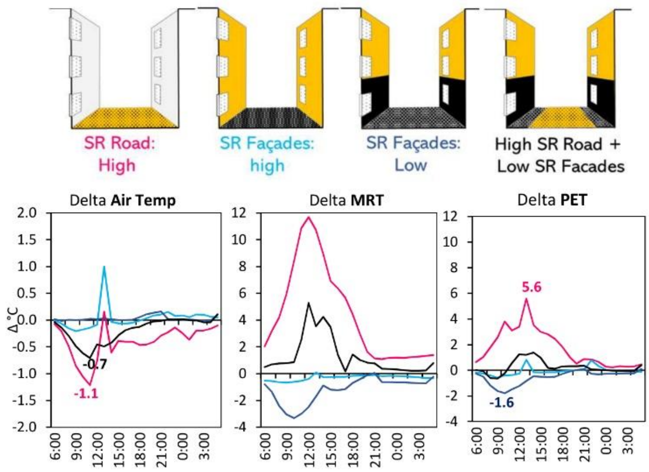

Figure 14 Hourly change in air temperature (black line), mean radiant temperature -MRT (pink line) and PET (clear blue line) at street level in point 1A (seeFigure 12) produced by the different reflectance scenarios. (2 columns picture)

ENVImet simulations showed that increasing the road reflectivity (SR Road: High) produces an increase in PET temperatures up to 5.6 ˚C during the hottest hour of the day. This happens because of the significant increase in MRT (up to almost + 12 ˚C) as a result of increase in reflected radiation at street level despite the reduction in peak air temperature (up to -1.1 ˚C). This result confirms what was found in other cities at lower latitudes [24,26,48]. This means that increasing the reflectivity of paving has a detrimental impact on outdoor thermal comfort in typical street canyon geometries (aspect ratio 0.75) in London, despite the positive impact on UCA and air temperature. Conversely, increasing the reflectance of façades (SR Facades: high) produces a very small reduction in MRT, while the impact on air temperature is negligible, resulting in a very limited improvement in PET (below 0.5˚C).

Surprisingly, the reduction of the façade reflectance (SR Facades: Low) reduces the PET temperatures, meaning it has a beneficial effect on outdoor thermal comfort. This happens thanks to the reduction of interreflections between surfaces, producing a reduction of the MRT and, consequently, an increase of radiation losses by the human body during the hottest hours of the day. The reduction in MRT is up to 3.3 ˚C, while the reduction in PET is up to 1.6 ˚C. It has to be noted that this scenario had the lowest impact on UCA among those analysed.

The last scenario analysed (High SR Road + Low SR Facades) has a lower reflectivity of the bottom part of the façades and a higher reflectivity of the road, except for the 2m pavement next to the façades. This combination produces a significant increase in UCA and it also avoids a detrimental impact on outdoor thermal comfort in the pavement area, where pedestrians walk. This probably happens because the increase in reflections from the road is balanced out by reduced reflections from the building façades. As a result, the MRT increase is limited to 5.3 ˚C and the PET increase to 1.2 ˚C, instead of +12 ˚C and +5.5 ˚C respectively seen in the high reflectivity road scenario (SR Road: high). However, none of the analysed reflective scenarios showed it possible to reach the same mitigation provided by vegetated areas with trees, where thermal comfort is found to be the best on such extremely hot days.

5.5. Impact of reflective scenarios on building indoor thermal conditions in urban canyons

Changing the solar reflectance of roads and façades affects the building indoor thermal environment by modifying two boundary conditions: the external surface temperature and the incident radiation on the façade. Increasing the solar reflectance of walls entails a reduction of external surface temperature, with positive impact on the indoor MRT and operative temperature. However, increasing the solar reflectance of roads and facades in urban canyons also produces an increase in the total incident radiation on the façades, which may have negative impact on indoor thermal comfort. ENVImet simulations showed that increasing the road reflectance from 0.19 to 0.5 led to an average 14% increase in daily incident radiation on the east-oriented façade analysed (considering the middle point of the façade). Conversely, increasing the reflectance of both canyon façades from 0.3 to 0.6 only causes a 3% increase in the incident radiation on the east façade.

The impact of such an increase in incident radiation on external surface temperature and indoor operative temperature is illustrated in Figure 15 for the east-oriented building, considering uninsulated and insulated wall constructions. The graph on top shows the indoor operative temperature and external surface temperature calculated by EnergyPlus for the baseline scenario. In both cases, indoor operative temperatures stayed above 30 ˚C throughout the day on the hottest day. The insulated model showed higher external surface temperatures, but slightly lower indoor operative temperature (approximately 1.5˚C lower on the hottest days).

The impact of reflective materials on external surface temperatures and operative temperature was analysed considering three scenarios as shown in Figure 15: reflective materials on the east façade (SR Facades: High (East)), reflecting materials on the facing (west-oriented) façade (SR Facades: High (West) and a reflective road (SR Road: High). The impact of these is illustrated in the middle and bottom graphs in Figure 15.

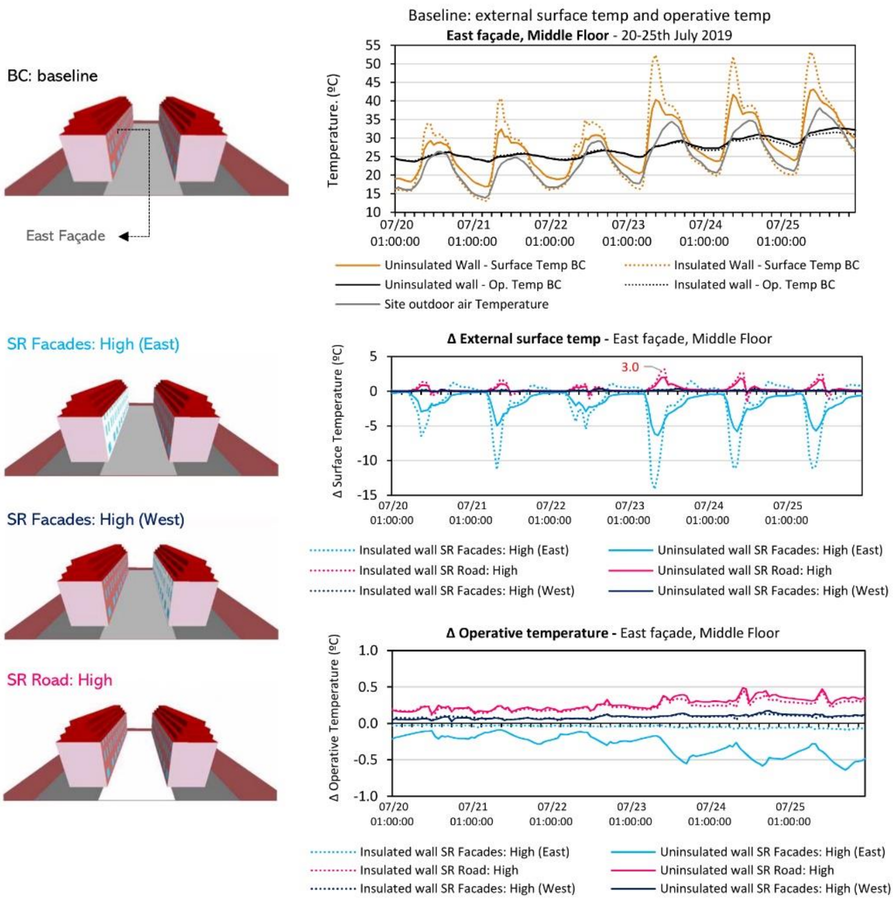

Figure 15 Indoor thermal conditions for the building in the baseline canyon model and impact of the two reflective scenarios with higher SR of road and façades. (2 columns picture)

The results showed that cool walls (SR Facades: High (East)) do allow external surface temperature to be reduced, even if solar availability is reduced in urban canyons. This has a positive impact on indoor thermal comfort, producing a reduction in indoor operative temperature up to 0.6˚C on the hottest day for walls without insulation. However, if walls have insulation, the beneficial effect of cool materials is lost because the heat transfer through the envelope is reduced, meaning that external surface temperatures take a marginal role on the indoor temperature.

Conversely, the results for the other two scenarios showed a negligible or negative impact on indoor thermal comfort.

The impact of increased solar reflectance of the opposite façade (SR Facades: High (West)) turned out to be negligible, with an impact on the indoor operative temperature limited to 0.2 ºC. On the other hand, increasing the reflectivity of the road (SR Road: High) increases the external walls' surface temperatures up to 3 ˚C for the insulated construction and 2 ˚C for the uninsulated one, thereby increasing the indoor operative temperature up to 0.5˚C on the hottest day. This increase in operative temperature would have an impact on the annual energy consumption of air-conditioned buildings. Its impact on thermal comfort would be negligible for typical days but would worsen conditions during days of high internal temperatures (i.e. above 28˚ C). These results suggest that increasing the albedo of roads may increase building overheating risk in typical residential areas of London.

6. Conclusion

The study investigated the multiple impacts of reflective materials on outdoor and indoor microclimates in London. The results highlighted that high reflectance materials may have an opposite impact on urban canyon albedo and outdoor thermal comfort depending on the urban canyon geometry. Increasing the solar reflectance of roads has the highest potential to increase urban canyon albedo in the typical canyon geometry of residential neighbourhoods in London (canyon aspect ratio around 0.75). However, it also worsens outdoor thermal comfort at street level, due to the increase of interreflections leading to a higher mean radiant temperature, despite the beneficial effect on air temperature. The effectiveness of this strategy to increase urban canyon albedo and reduce urban air temperature is also drastically reduced in deeper canyons, where instead, façade reflectivity has more potential in increasing urban canyon albedo. Increasing the façades' reflectivity does not affect air temperature, given the reduced solar availability on vertical surfaces in urban canyons. However, decreasing the reflectivity of the bottom part of façades seems to have a positive impact on outdoor thermal comfort, by reducing solar reflections towards pedestrians and mean radiant temperature. For this reason, the combination of higher road reflectivity and lower façades reflectivity in the bottom part would be the best strategy for residential areas in London to mitigate the UHI while avoiding detrimental impact on street-level thermal comfort. The results also showed that none of the analysed reflective scenarios had the same mitigation potential of vegetated areas with trees, where thermal comfort is found to be the best on extremely hot days.

Increasing the reflectivity of road and walls has a reduced, but opposite, impact on indoor operative temperatures in London. Cool walls have a slight positive effect in uninsulated buildings, which becomes negligible in insulated ones due to the reduced heat transfer through the envelope. Conversely, high reflectance on roads has a negative impact on indoor operative temperatures of both insulated and uninsulated buildings, entailing some risk of increasing the building cooling loads and heat stress.

The analysis presented highlighted the varying impact of reflective materials in urban settings. The results can be used as preliminary guidelines and rules of thumb for architects and planners for a more informed use of high and low reflectance materials to improve the urban microclimate and thermal comfort in London and other cities of similar latitudes and canyon geometries.

7. Acknowledgements

This work was funded by EPSRC UK under the project 'Urban albedo computation in high latitude locations: An experimental approach' (EP/P02517X/1).

8. Appendix

ENVImet model specification and additional outputs

The 3D view and materials specification of the detailed ENVImet model are reported in Figure 16 and Table 4.

Figure 16 Left: Aerial view of the case study area and corresponding detailed ENVImet model. Right: view of the physical model and corresponding simplified ENVImet model (2 columns picture)

Table 4. ENVImet base model material reflectivity and distribution

Urban canyon		K_Rd		S_Rd		L_Rd	
Façade materials (divided by orientation)		ESE	WNW	SSW	NNE	SSE	NNW
Red Bricks	SR= 0.32	9%	40%	-	69%	8%	4%
Yellow bricks	SR= 0.43	25%	-	33%	-	31%	33%
Painted brick	SR= 0.2	9%	-	-	-	-	-
Dark paints	SR= 0.08	-	-	3%	1%	-	-
White painted bricks	SR= 0.56	38%	35%	40%	17%	33%	42%
Clear glass	SR= 0.05	19%	25%	24%	13%	28%	22%
Road materials							
Tarmac and concrete paving	SR= 0.19	100%		100%		100%	

The spatial distribution of solar reflections calculated by ENVImet for the case study area is reported in Figure 17. The impact of urban geometry and vegetation on the spatial variability of solar reflection is clear from ENVImet results. It is observed that despite having similar geometry and material distribution, the reflected radiation at the eaves level is reduced in point 2 compared to points 1 and 3. This happens because point 2 is located on top of the tree canopy. This highlights the relevant role played by vegetation on UA which was not investigated in this study.

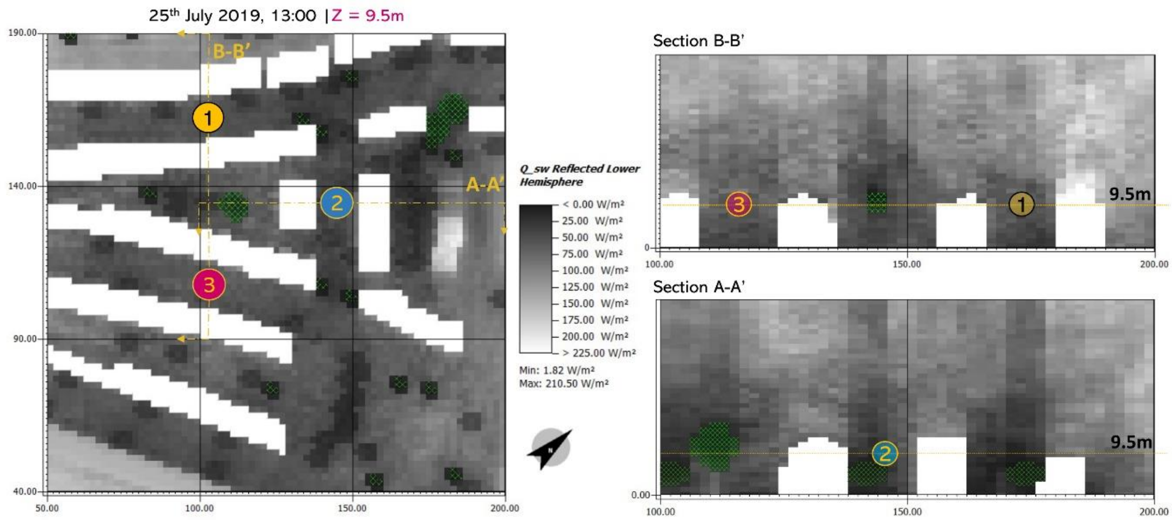

Figure 17 Baseline model: ENVImet solar reflections at the eaves level (9.5m above ground level) (2 columns picture)

The spatial distribution of air temperature and MRT during the heatwave peak are reported in Figure 18 and Figure 19.

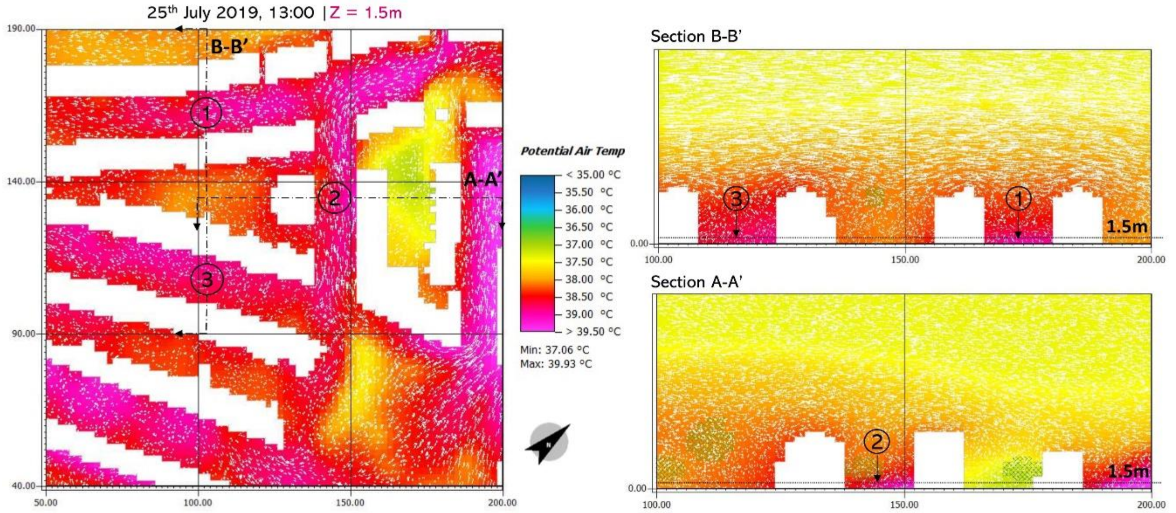

Figure 18 Baseline model | Air temperature and wind vectors during the heatwave peak (25th of July at 13:00 UTC) *(2 columns picture)*

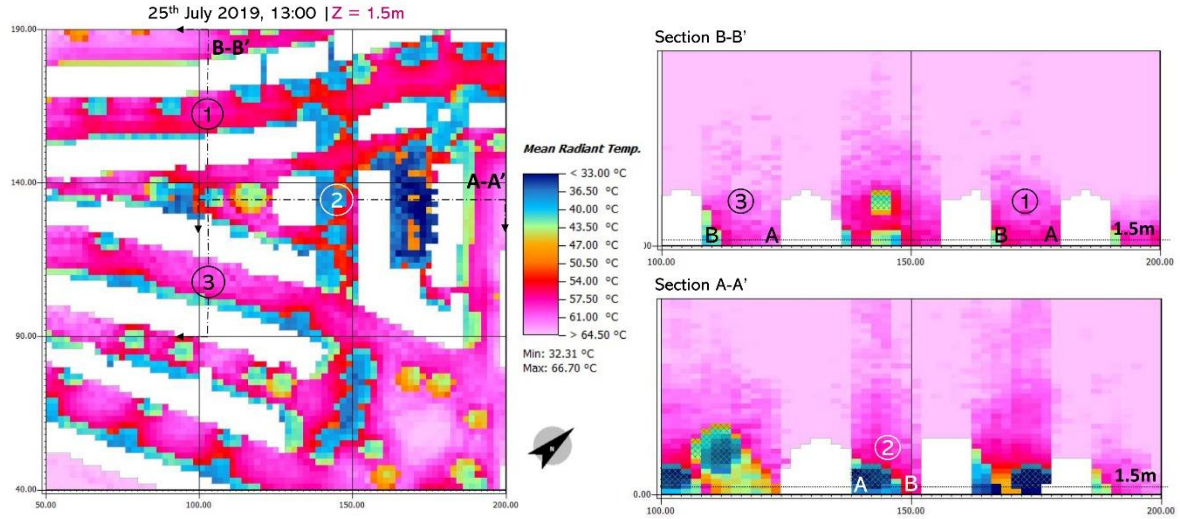

Figure 19 Baseline model | Mean radiant temperature during the heatwave peak (25th of July at 13:00 UTC) *(2 columns picture)*

The figures show that the MRT has a higher range of variation than air temperature, being significantly lower in the areas in shadow and with more vegetation (courtyards). The vertical sections show that both air temperature and MRT are higher between buildings than above roof level, probably due to the effect of reduced wind speed.

Performance of the IVS algorithm in versions V4.4.5 and 4.4.6

The accuracy of ENVImet in estimating the reflected radiation within and above urban canyons showed substantial differences depending on the version. The last version of the IVS algorithm (ENVImet V4.4.6) showed much higher accuracy compared to the previous version (ENVImet 4.4.5) when compared to the field measurements (i.e. reflections within urban canyons). The previous version largely overestimated the reflected radiation in some of the points, as discussed in a previous work of the authors [65].

The comparison between the reflected radiation measured on the physical model and computed by ENVImet version 4.4.5 and 4.4.6 are shown in Figure 20. The results using the IVS algorithm of version 4.4.5 showed a clear overestimation of the reflected radiation in point 1, starting from noon and lasting until sunset, resulting in significant overestimations of the hourly UA in the afternoon and the daily UA compared to measurements. The new version 4.4.6 instead shows a more realistic trend of reflections on top of the model, without an unrealistic increase in the afternoon compared to morning.

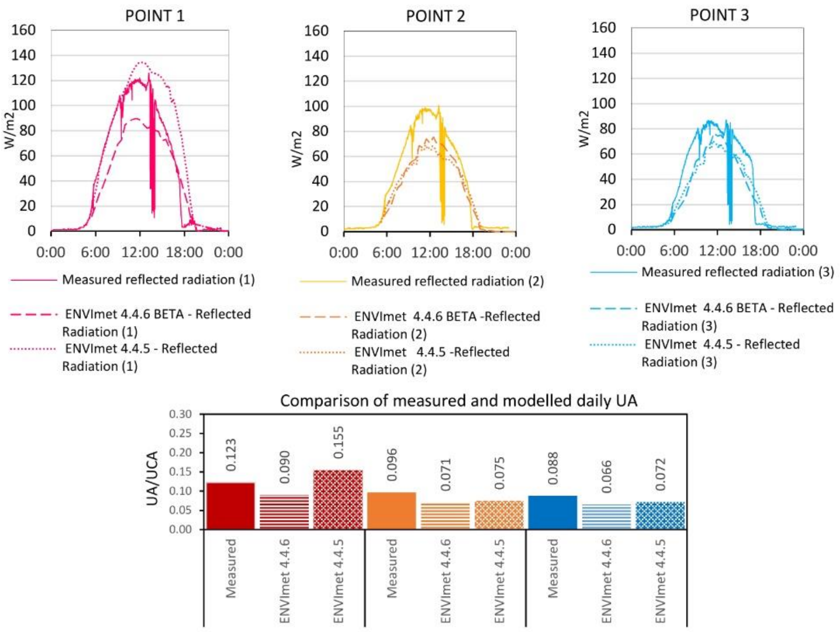

Figure 20 TOP: Hourly comparison of the reflected radiation calculated by ENVImet versions 4.4.5 and 4.4.6 and measured on the physical model in different points on the 22^{nd} of June 2019. Bottom: Comparison of measured and modelled daily UA (point 1) and UCA (points 2 and 3) (2 columns picture)

In light of these results, the IVS version 4.4.6 is deemed more reliable because the trend of the reflected radiation is the same as the measured data and the underestimation is consistent in percentage over the time and across the model. Conversely, the reflected radiation calculated by version 4.4.5 on top of the model (point 1) showed good agreement with the measurements from sunrise to noon and large overestimation after noon (see graph on the left in Figure 20). There is no physical explanation for such asymmetry in reflected radiation before and after noon, and for this reason this version was discarded.

9. References

[1] W. Miller, A. Machard, E. Bozonnet, N. Yoon, D. Qi, C. Zhang, A. Liu, A. Sengupta, J. Akander, A. Hayati, M. Cehlin, O.B. Kazanci, R. Levinson, Conceptualising a resilient cooling system: A socio-technical approach, City Environ. Interact. 11 (2021) 100065. https://doi.org/10.1016/j.cacint.2021.100065.

[2] S. Attia, R. Levinson, E. Ndongo, P. Holzer, O. Berk Kazanci, S. Homaei, C. Zhang, B.W. Olesen, D. Qi, M. Hamdy, P. Heiselberg, Resilient cooling of buildings to protect against heat waves and power outages: Key concepts and definition, Energy Build. 239 (2021) 110869. https://doi.org/10.1016/j.enbuild.2021.110869.

[3] World Bank, World DataBank, Urban Popul. (2019). https://data.worldbank.org/indicator/SP.URB.TOTL.IN.ZS?view=chart (accessed December 18, 2019).

[4] M. Kolokotroni, X. Ren, M. Davies, A. Mavrogianni, London's urban heat island: Impact on current and future energy consumption in office buildings, Energy Build. 47 (2012) 302–311. https://doi.org/10.1016/j.enbuild.2011.12.019.

[5] A. Mavrogianni, M. Davies, M. Batty, S.E. Belcher, S.I. Bohnenstengel, D. Carruthers, Z. Chalabi, B. Croxford, C. Demanuele, S. Evans, R. Giridharan, J.N. Hacker, I.G. Hamilton, C. Hogg, J. Hunt, M. Kolokotroni, C. Martin, J. Milner, I. Rajapaksha, I. Ridley, J.P. Steadman, J. Stocker, P. Wilkinson, Z. Ye, The comfort, energy and health implications of London's urban heat island, Build. Serv. Eng. Res. Technol. 32 (2011) 35–52. https://doi.org/10.1177/0143624410394530.

[6] D. Li, E. Bou-Zeid, Synergistic Interactions between Urban Heat Islands and Heat Waves: The Impact in Cities Is Larger than the Sum of Its Parts, J. Appl. Meteorol. Climatol. 52 (2013) 2051–2064. https://doi.org/10.1175/JAMC-D-13-02.1.

[7] D. Founda, F. Pierros, M. Petrakis, C. Zerefos, Interdecadal variations and trends of the Urban Heat Island in Athens (Greece) and its response to heat waves, Atmos. Res. 161–162 (2015)

1–13. https://doi.org/10.1016/j.atmosres.2015.03.016.

[8] Public Health England, Heatwave plan for England, (2019).

[9] T.R. Oke, G. Mills, A. Christen, J.A. Voogt, Urban Climates, Cambridge University Press, 2017. https://doi.org/10.1017/9781139016476.

[10] A. Salvati, P. Monti, H. Coch Roura, C. Cecere, Climatic performance of urban textures: Analysis tools for a Mediterranean urban context, Energy Build. 185 (2019) 162–179. https://doi.org/10.1016/j.enbuild.2018.12.024.

[11] G. Mills, J. Futcher, I. Stewart, The Urban Heat Island: Its Energetic Basis and Management, in: Urban Microclimate Modelling for Comfort and Energy Studies (Palme and Salvati eds.), Springer Nature, 2021.

[12] E. Erell, D. Pearlmutter, T. Williamson, Urban Microclimate. Designing the space between buildings, Earthscan publishing, London, 2011.

[13] E.S. Krayenhoff, A.M. Broadbent, L. Zhao, M. Georgescu, A. Middel, J.A. Voogt, A. Martilli, D.J. Sailor, E. Erell, Cooling hot cities: a systematic and critical review of the numerical modelling literature, Environ. Res. Lett. 16 (2021). https://doi.org/10.1088/1748-9326/abdcf1.

[14] H. Akbari, D. Kolokotsa, Three decades of urban heat islands and mitigation technologies research, Energy Build. 133 (2016) 834–852. https://doi.org/10.1016/j.enbuild.2016.09.067.

[15] M. Santamouris, Cooling the cities - A review of reflective and green roof mitigation technologies to fight heat island and improve comfort in urban environments, Sol. Energy. 103 (2014) 682–703. https://doi.org/10.1016/j.solener.2012.07.003.

[16] D.-D. Kolokotsa, G. Giannariakis, K. Gobakis, G. Giannarakis, Cool roofs and cool pavements application in Acharnes , Greece, Sustain. Cities Soc. 37 (2018) 466–474. https://doi.org/10.1016/j.scs.2017.11.035.

[17] H. Taha, R. Levinson, A. Mohegh, H. Gilbert, G. Ban-Weiss, S. Chen, Air-temperature response to neighborhood-scale variations in albedo and canopy cover in the real world: Fine-resolution meteorological modeling and mobile temperature observations in the Los Angeles climate archipelago, Climate. 6 (2018). https://doi.org/10.3390/cli6020053.

[18] A.L. Pisello, V.L. Castaldo, C. Piselli, C. Fabiani, F. Cotana, Thermal performance of coupled

cool roof and cool façade: Experimental monitoring and analytical optimization procedure, Energy Build. 157 (2017) 35–52. https://doi.org/10.1016/j.enbuild.2017.04.054.

[19] M. Kolokotroni, E. Shittu, T. Santos, L. Ramowski, A. Mollard, K. Rowe, E. Wilson, J. Pereira, D.B. Filho, D. Novieto, Cool roofs: high tech low cost solution for energy efficiency and thermal comfort in low rise low income houses in high solar radiation countries, Energy Build. 176 (2018) 58–70. https://doi.org/10.1016/j.enbuild.2018.07.005.

[20] P.J. Rosado, R. Levinson, Potential benefits of cool walls on residential and commercial buildings across California and the United States : Conserving energy , saving money , and reducing emission of greenhouse gases and air pollutants, Energy Build. 199 (2019) 588–607. https://doi.org/10.1016/j.enbuild.2019.02.028.

[21] R. Guo, Y. Gao, C. Zhuang, P. Heiselberg, R. Levinson, Optimization of cool roof and night ventilation in office buildings : A case study in Xiamen , China, Renew. Energy. 147 (2020) 2279–2294. https://doi.org/10.1016/j.renene.2019.10.032.

[22] M. Zinzi, Exploring the potentialities of cool facades to improve the thermal response of Mediterranean residential buildings, Sol. Energy. 135 (2016) 386–397. https://doi.org/10.1016/j.solener.2016.06.021.

[23] Y. Qin, Urban canyon albedo and its implication on the use of reflective cool pavements, Energy Build. 96 (2015) 86–94. https://doi.org/10.1016/j.enbuild.2015.03.005.

[24] A. Middel, V.K. Turner, F.A. Schneider, Y. Zhang, M. Stiller, Solar reflective pavements-A policy panacea to heat mitigation?, Environ. Res. Lett. 15 (2020). https://doi.org/10.1088/1748-9326/ab87d4.

[25] N. Nazarian, N. Dumas, J. Kleissl, L. Norford, Effectiveness of cool walls on cooling load and urban temperature in a tropical climate, Energy Build. 187 (2019) 144–162. https://doi.org/10.1016/j.enbuild.2019.01.022.

[26] E. Erell, D. Pearlmutter, D. Boneh, P. Bar, Effect of high-albedo materials on pedestrian heat stress in urban street canyons, Urban Clim. 10 (2014) 367–386. https://doi.org/10.1016/j.uclim.2013.10.005.

[27] X. Yang, Y. Li, The impact of building density and building height heterogeneity on average

urban albedo and street surface temperature, Build. Environ. 90 (2015) 146–156. https://doi.org/10.1016/j.buildenv.2015.03.037.

[28] K. Fortuniak, Numerical estimation of the effective albedo of an urban canyon, Theor. Appl. Climatol. 91 (2008) 245–258. https://doi.org/10.1007/s00704-007-0312-6.

[29] D. Groleau, P.G. Mestayer, Urban Morphology Influence on Urban Albedo: A Revisit with the Solene Model, Boundary-Layer Meteorol. 147 (2013) 301–327. https://doi.org/10.1007/s10546-012-9786-6.

[30] A. Kondo, M. Ueno, A. Kaga, K. Yamaguchi, The influence of urban canopy configuration on urban albedo, Boundary-Layer Meteorol. 100 (2001) 225–242. https://doi.org/10.1023/A:1019243326464.

[31] K. Steemers, N. Baker, D. Crowther, J. Dubiel, M. Nikolopoulou, Radiation absorption and urban texture, Build. Res. Inf. 26 (1998) 103–112. https://doi.org/10.1080/096132198370029.

[32] X. Li, J. Peoples, Z. Huang, Z. Zhao, J. Qiu, X. Ruan, Full Daytime Sub-ambient Radiative Cooling in Commercial-like Paints with High Figure of Merit, Cell Reports Phys. Sci. 1 (2020) 100221. https://doi.org/10.1016/j.xcrp.2020.100221.

[33] W. Pawlak, K. Fortuniak, Applcation of physical model to study effective albedo of the urban canyon, in: Fifth Int. Conf. Urban Clim., Lodz, Poland, 2003: pp. 5–8.

[34] M. Aida, Urban albedo as a function of the urban structure - a model experiment, Boundary-Layer Meteorol. 23 (1982) 405–413.

[35] Y. Qin, K. Tan, D. Meng, F. Li, Theory and procedure for measuring the solar reflectance of urban prototypes, Energy Build. 126 (2016) 44–50. https://doi.org/10.1016/j.enbuild.2016.05.026.

[36] A.J. Arnfield, An approach to the estimation of the surface radiative properties and radiation budgets of cities, Phys. Geogr. 3 (1982) 97–122. https://doi.org/10.1080/02723646.1982.10642221.

[37] E. Morini, B. Castellani, A. Presciutti, E. Anderini, M. Filipponi, A. Nicolini, F. Rossi, Experimental analysis of the effect of geometry and façade materials on urban district's equivalent albedo, Sustain. 9 (2017). https://doi.org/10.3390/su9071245.

[38] M. Aida, K. Gotoh, Urban albedo as a function of the urban structure — A two-dimensional numerical simulation, Boundary-Layer Meteorol. 23 (1982) 415–424.

[39] A. Kondo, M. Ueno, A. Kaga, K. Yamaguchi, The Influence of Urban Canopy Configuration on Urban Albedo, Boundary-Layer Meteorol. (2001) 225–242.

[40] E. Morini, A.G. Touchaei, F. Rossi, F. Cotana, H. Akbari, Evaluation of albedo enhancement to mitigate impacts of urban heat island in Rome (Italy) using WRF meteorological model, Urban Clim. 24 (2018) 551–566. https://doi.org/10.1016/j.uclim.2017.08.001.

[41] E.S. Krayenhoff, J.A. Voogt, Impacts of urban albedo increase on local air temperature at daily-annual time scales: Model results and synthesis of previous work, J. Appl. Meteorol. Climatol. 49 (2010) 1634–1648. https://doi.org/10.1175/2010JAMC2356.1.

[42] M. Santamouris, A. Synnefa, T. Karlessi, Using advanced cool materials in the urban built environment to mitigate heat islands and improve thermal comfort conditions, Sol. Energy. 85 (2011) 3085–3102. https://doi.org/10.1016/j.solener.2010.12.023.

[43] M. Santamouris, D. Kolokotsa, Urban climate mitigation techniques, 2016. https://doi.org/10.4324/9781315765839.

[44] Z. Jandaghian, H. Akbari, The effect of increasing surface albedo on urban climate and air quality: A detailed study for Sacramento, Houston, and Chicago, Climate. 6 (2018). https://doi.org/10.3390/cli6020019.

[45] A. Mohegh, R. Levinson, H. Taha, H. Gilbert, J. Zhang, Y. Li, T. Tang, G.A. Ban-Weiss, Observational evidence of neighborhood scale reductions in air temperature associated with increases in roof albedo, Climate. 6 (2018). https://doi.org/10.3390/cli6040098.

[46] G. Kyriakodis, M. Santamouris, Urban Climate Using reflective pavements to mitigate urban heat island in warm climates - Results from a large scale urban mitigation project, Urban Clim. 24 (2018) 326–339. https://doi.org/10.1016/j.uclim.2017.02.002.

[47] F. Salata, I. Golasi, A. De Lieto, R. De Lieto, How high albedo and traditional buildings ' materials and vegetation affect the quality of urban microclimate . A case study, Energy Build. 99 (2015) 32–49. https://doi.org/10.1016/j.enbuild.2015.04.010.

[48] N.L. Alchapar, E.N. Correa, The use of reflective materials as a strategy for urban cooling in

an arid “OASIS” city, Sustain. Cities Soc. 27 (2016) 1–14. https://doi.org/10.1016/j.scs.2016.08.015.

[49] B.H. Lynn, T.N. Carlson, C. Rosenzweig, R. Goldberg, L. Druyan, J. Cox, S. Gaffin, L. Parshall, K. Civerolo, A modification to the NOAH LSM to simulate heat mitigation strategies in the New York City metropolitan area, J. Appl. Meteorol. Climatol. 48 (2009) 199–216. https://doi.org/10.1175/2008JAMC1774.1.

[50] D. Pearlmutter, P. Berliner, E. Shaviv, Physical modeling of pedestrian energy exchange within the urban canopy, Build. Environ. 41 (2006) 783–795. https://doi.org/10.1016/j.buildenv.2005.03.017.

[51] P. Hoppe, The physiological equivalent temperature – a universal index for the biometeorological assessment of the thermal environment, Int. J. Biometeorol. 43 (1999) 71–75.

[52] A. Synnefa, M. Santamouris, H. Akbari, Estimating the effect of using cool coatings on energy loads and thermal comfort in residential buildings in various climatic conditions, Energy Build. 39 (2007) 1167–1174.

[53] S. Boixo, M. Diaz-vicente, A. Colmenar, M. Alonso, Potential energy savings from cool roofs in Spain and Andalusia, Energy. 38 (2012) 425–438. https://doi.org/10.1016/j.energy.2011.11.009.

[54] A.L. Pisello, F. Cotana, The thermal effect of an innovative cool roof on residential buildings in Italy : Results from two years of continuous monitoring, Energy Build. 69 (2014) 154–164. https://doi.org/10.1016/j.enbuild.2013.10.031.

[55] C. Romeo, M. Zinzi, Impact of a cool roof application on the energy and comfort performance in an existing non-residential building . A Sicilian case study, Energy Build. 67 (2013) 647–657. https://doi.org/10.1016/j.enbuild.2011.07.023.

[56] M. Zinzi, Cool materials and cool roofs: Potentialities in Mediterranean buildings, Adv. Build. Energy Res. 4 (2010) 201–266. https://doi.org/10.3763/aber.2009.0407.

[57] R. Levinson, Using solar availability factors to adjust cool-wall energy savings for shading and reflection by neighboring buildings, Sol. Energy. 180 (2019) 717–734.

https://doi.org/10.1016/j.solener.2019.01.023.

[58] X. Xu, H. AzariJafari, J. Gregory, L. Norford, R. Kirchain, An integrated model for quantifying the impacts of pavement albedo and urban morphology on building energy demand, Energy Build. 211 (2020). https://doi.org/10.1016/j.enbuild.2020.109759.

[59] N. Yaghoobian, J. Kleissl, Effect of reflective pavements on building energy use, Urban Clim. 2 (2012) 25–42. https://doi.org/10.1016/j.uclim.2012.09.002.

[60] C. Colucci, L. Mauri, A. Vallati, About the shortwave multiple reflections in an urban street, 05004 (2018) 1–7.

[61] A. Salvati, M. Kolokotroni, Microclimate Data For Building Energy Modelling : Study On ENVI-Met Forcing Data, in: V. Corrado, A. Gasparella (Eds.), Proc. 16th IBPSA Conf., Rome, Italy, Sept. 2-4, 2019, 2019: pp. 3361–3368.

[62] H. Simon, T. Sinsel, M. Bruse, Advances in Simulating Radiative Transfer in Complex Environments, Appl. Sci. 11 (2021) 5449. https://doi.org/10.3390/app11125449.

[63] Ordnance Survey, OS MasterMap Topography Layer, (2018). https://www.ordnancesurvey.co.uk/business-government/products/mastermap-building.

[64] S. Kotthaus, T.E.L. Smith, M.J. Wooster, C.S.B. Grimmond, Derivation of an urban materials spectral library through emittance and reflectance spectroscopy, ISPRS J. Photogramm. Remote Sens. 94 (2014) 194–212. https://doi.org/10.1016/j.isprsjprs.2014.05.005.

[65] A. Salvati, M. Kolokotroni, Impact of urban albedo on microclimate and thermal comfort over a heat wave event in London, in: S. Roaf, F. Nicol, W. Finlayson (Eds.), Wind. 2020 Resilient Comf. Proc., Windsor, UK, 2020: pp. 566–578. https://windsorconference.com/wp-content/uploads/2020/05/WC2020_Proceedings_final_compressed.pdf.